Relativistic Radiative Flow in a Luminous Disk II

Jun FUKUE and Chizuru AKIZUKI

Astronomical Institute, Osaka Kyoiku University, Asahigaoka, Kashiwara, Osaka 582-8582

fukue@cc.osaka-kyoiku.ac.jp

Abstract

Radiatively driven transfer flow perpendicular to a luminous disk is examined in the relativistic regime of $(v/c)^2$, while taking into account the gravity of the central object. The flow is assumed to be vertical, and the gas pressure as well as the magnetic field are ignored. Using a velocity-dependent variable Eddington factor, we can solve the rigorous equations of the relativistic radiative flow accelerated up to *relativistic* speeds. For sufficiently luminous cases, the flow resembles the case without gravity. For less-luminous or small initial radius cases, however, the flow velocity decreases due to gravity. Application to a supercritical accretion disk with mass loss is briefly discussed.

Key words: accretion, accretion disks — astrophysical jets — radiative transfer — relativity

1. Introduction

Mass outflow from a luminous disk is a clue to the formation mechanism of astrophysical jets and winds in the active objects. In particular, in a supercritical accretion disk, the disk local luminosity exceeds the Eddington one, and mass loss from a disk surface driven by radiation pressure would take place (see Kato et al. 1998 for a review of accretion disks).

So far, radiatively driven outflows from a luminous disk have been extensively studied by many researchers (Bisnovatyi-Kogan, Blinnikov 1977; Katz 1980; Icke 1980; Melia, Königl 1989; Misra, Melia 1993; Tajima, Fukue 1996, 1998; Watarai, Fukue 1999; Hirai, Fukue 2001; Fukue et al. 2001; Orihara, Fukue 2003), and by numerical simulations (Eggum et al. 1985, 1988; Okuda 2002; Ohsuga et al. 2005; Ohsuga 2006). In almost all of these studies, however, the luminous disk was treated as an external radiation source, and radiation transfer in the flow was not solved.

Radiation transfer in the disk, on the other hand, was investigated in relation to the structure of a static disk atmosphere and the spectral energy distribution from the disk surface (e.g., Meyer, Meyer-Hofmeister 1982; Cannizzo, Wheeler 1984; Shaviv, Wehrse 1986; Adam et al. 1988; Hubeny 1990; Ross et al. 1992; Artemova et al. 1996; Hubeny, Hubeny 1997, 1998; Hubeny et al. 2000, 2001; Davis et al. 2005; Hui et al. 2005). In these studies, however, the vertical movement and the mass loss were not considered.

Recently, mass outflow as well as radiation transfer has been examined for the first time in the subrelativistic (Fukue 2005a, 2006a) and fully relativistic cases (Fukue 2005b). In the latter case, it is pointed out some singular behavior inherent in relativistic radiative flow (e.g., Turolla, Nobili 1988; Turolla et al. 1995; Dullemond 1999). When the gaseous flow is radiatively accelerated up to the relativistic regime, the velocity gradient becomes very large in the direction of the flow. As a result, the radiative diffusion may become *anisotropic* in the comoving frame of the gas. Hence, in a flow that is accelerated from subrelativistic to relativistic regimes, the Eddington factor should be different from 1/3, even in the

optically thick diffusion limit.

In order to avoid the singular behavior of such a relativistic regime, for a plane-parallel case, Fukue (2006b) proposed a *velocity-dependent Eddington factor*, which depends on the flow velocity v,

$$f(\beta) = \frac{1 + 2\beta}{3}, \tag{1}$$

where $\beta = v/c$. In Fukue (2006b) this form (1) was adopted as the simplest one among various forms, which satisfy several necessary conditions to avoid a singularity. Physically speaking, this form (1) can be interpreted as follows. In the high-velocity regime, where the radiative diffusion may become anisotropic in a comoving frame, the 'apparent' optical depth, τ, would be on the order of

$$1 + \tau = \frac{1}{\beta}. \tag{2}$$

That is, as the flow is accelerated and approaches the speed of light, the optical depth becomes zero (outward *peaking*). In this case, form (1) can be read as

$$f(\tau) = \frac{3 + \tau}{3 + 3\tau}, \tag{3}$$

which recovers a similar form of a usual variable Eddington factor (see, e.g., Tamazawa et al. 1975). Hence, the applicability and accuracy of form (1) from a low-speed regime to a high-speed one would be similar to those of a variable Eddington factor from an optically thick regime to an optically thin one.

Similarly, for a spherically symmetric case, Akizuki and Fukue (2006) proposed a variable Eddington factor, that depends on the flow velocity, β, as well as the optical depth, τ:

$$f(\tau, \beta) = \frac{\gamma(1 + \beta) + \tau}{\gamma(1 + \beta) + 3\tau}, \tag{4}$$

where $\gamma \ (= 1/\sqrt{1 - \beta^2})$ is the Lorentz factor.

In Fukue (2006b), the plane-parallel case was examined as an example, although the gravity of the central object was

ignored for simplicity. In this paper, we thus consider the radiatively driven vertical outflow—*moving photosphere*—in a luminous flat disk within the framework of radiation transfer in the relativistic regime using $f(\beta)$, while taking into account the gravity of the central object, although the gas pressure is ignored.

In the next section we describe the basic equations in the vertical direction. In section 3 we show our numerical examination of the radiative flow. In section 4 we briefly apply the present model to the case of a supercritical accretion disk. The final section is devoted to concluding remarks.

2. Basic Equations and Boundary Conditions

Let us suppose a luminous flat disk, inside of which gravitational or nuclear energy is released via viscous heating or other processes. The radiation energy is transported in the vertical direction, and the disk gas, itself, also moves in the vertical direction due to the action of radiation pressure. For simplicity, in the present paper, the radiation field is considered to be sufficiently intense that the gas pressure can be ignored: tenuous cold normal plasmas in the super-Eddington disk, cold pair plasmas in the sub-Eddington disk, or dusty plasmas in the sub-Eddington disk. As for the order of the flow velocity v, we consider the fully relativistic regime, where the terms are retained up to the second order of (v/c).

2.1. Basic Equations

Under these assumptions, the radiation hydrodynamic equations for steady vertical (z) flows without rotation are described as follows (Kato et al. 1998; Fukue 2006b).

The continuity equation is

$$\rho c u = J \quad (= \text{const.}), \tag{5}$$

where ρ is the proper gas density, u the vertical four velocity, J the mass-loss rate per unit area, and c the speed of light. The four-velocity u is related to the proper three-velocity v by $u = \gamma v/c$, where γ is the Lorentz factor, $\gamma = \sqrt{1 + u^2} = 1/\sqrt{1 - (v/c)^2}$.

The equation of motion is

$$c^2 u \frac{du}{dz} = -\frac{GMz}{(R - r_{\rm g})^2 R}$$
$$+ \frac{\kappa_{\rm abs} + \kappa_{\rm sca}}{c} \left[F\gamma(1 + 2u^2) - (cE + cP)\gamma^2 u \right], \tag{6}$$

where M is the mass of the central object, $R = \sqrt{r^2 + z^2}$, r being the radius, $r_{\rm g} \, (= 2GM/c^2)$ is the Schwarzschild radius, $\kappa_{\rm abs}$ and $\kappa_{\rm sca}$ are the absorption and scattering opacities (gray), defined in the comoving frame, E the radiation energy density, F the radiative flux, and P the radiation pressure observed in the inertial frame. The first term in the square brackets on the right-hand side of equation (6) means the radiatively driven force, which is modified to the order of u^2, whereas the second term is the radiation drag force, which is also modified, but roughly proportional to the velocity. As for the gravity, we adopt the pseudo-Newtonian potential (Paczyński, Wiita 1980).

When the gas pressure is ignored, the advection terms of the

energy equation are dropped (cf. Kato et al. 1998), and heating is balanced with the radiative terms,

$$0 = q^+ - \rho \left(j - \kappa_{\rm abs} cE\gamma^2 - \kappa_{\rm abs} cPu^2 + 2\kappa_{\rm abs} F\gamma u \right), \tag{7}$$

where q^+ is the internal heating and j is the emissivity defined in the comoving frame. In this equation (7), the third and fourth terms on the right-hand side appear in the relativistic regime.

For radiation fields, the zeroth-moment equation becomes

$$\frac{dF}{dz} = \rho\gamma \left[j - \kappa_{\rm abs} cE + \kappa_{\rm sca}(cE + cP)u^2 \right.$$
$$\left. + \kappa_{\rm abs} Fu/\gamma - \kappa_{\rm sca} F(1 + v^2/c^2)\gamma u \right]. \tag{8}$$

The first-moment equation is

$$\frac{dP}{dz} = \frac{\rho\gamma}{c} \left[\frac{u}{\gamma} j - \kappa_{\rm abs} F + \kappa_{\rm abs} cP \frac{u}{\gamma} \right.$$
$$\left. - \kappa_{\rm sca} F(1 + 2u^2) + \kappa_{\rm sca}(cE + cP)\gamma u \right]. \tag{9}$$

In order to close moment equations for radiation fields, we need some closure relation. Instead of the usual Eddington approximation, we here adopt a *velocity-dependent* variable Eddington factor, $f(\beta)$,

$$P_0 = f(\beta)E_0, \tag{10}$$

in the comoving frame, where P_0 and E_0 are the quantities in the comoving frame. If we adopt this form (10) as the closure relation in the comoving frame, the transformed closure relation in the inertial frame is

$$cP(1 + u^2 - fu^2) = cE(f\gamma^2 - u^2) + 2F\gamma u(1 - f), \tag{11}$$

or equivalently,

$$cP(1 - f\beta^2) = cE(f - \beta^2) + 2F\beta(1 - f). \tag{12}$$

As a form of the function $f(\beta)$ we adopt the simplest one,

$$f(\beta) = \frac{1}{3} + \frac{2}{3}\beta, \tag{13}$$

for a plane-parallel geometry (Fukue 2006b; cf. Akizuki and Fukue 2006 for a spherically symmetric geometry).

Eliminating j and E with the help of equations (7) and (11), equations (6), (8), and (9) become

$$c^2 u \frac{du}{dz} = -\frac{c^2 r_{\rm g} z}{2(R - r_{\rm g})^2 R}$$
$$+ \frac{\kappa_{\rm abs} + \kappa_{\rm sca}}{c} \gamma \frac{F(f\gamma^2 + u^2) - cP(1 + f)\gamma u}{f\gamma^2 - u^2}, \tag{14}$$

$$\frac{dF}{dz} = q^+ \gamma$$
$$- \rho(\kappa_{\rm abs} + \kappa_{\rm sca}) u \frac{F(f\gamma^2 + u^2) - cP(1 + f)\gamma u}{f\gamma^2 - u^2}, \tag{15}$$

$$\frac{dP}{dz} = q^+ \frac{u}{c}$$
$$- \rho \frac{\kappa_{\rm abs} + \kappa_{\rm sca}}{c} \gamma \frac{F(f\gamma^2 + u^2) - cP(1 + f)\gamma u}{f\gamma^2 - u^2}. \tag{16}$$

Introducing the optical depth by

$$d\tau = -(\kappa_{\mathrm{abs}} + \kappa_{\mathrm{sca}})\rho\,dz, \tag{17}$$

and using continuity equation (5), equations (14)–(17) are rearranged as

$$c^2 J \frac{du}{d\tau} = \frac{c}{\kappa_{\mathrm{abs}} + \kappa_{\mathrm{sca}}} \frac{c^2 r_{\mathrm{g}} z}{2(R - r_{\mathrm{g}})^2 R}$$
$$- \gamma \frac{F(f\gamma^2 + u^2) - cP(1 + f)\gamma u}{f\gamma^2 - u^2}, \tag{18}$$

$$J \frac{dz}{d\tau} = -\frac{cu}{\kappa_{\mathrm{abs}} + \kappa_{\mathrm{sca}}}, \tag{19}$$

$$\frac{dF}{d\tau} = -\frac{q^+}{(\kappa_{\mathrm{abs}} + \kappa_{\mathrm{sca}})\rho}$$
$$+ u \frac{F(f\gamma^2 + u^2) - cP(1 + f)\gamma u}{f\gamma^2 - u^2}, \tag{20}$$

$$c \frac{dP}{d\tau} = -\frac{q^+}{(\kappa_{\mathrm{abs}} + \kappa_{\mathrm{sca}})\rho} \frac{J}{c}$$
$$+ \gamma \frac{F(f\gamma^2 + u^2) - cP(1 + f)\gamma u}{f\gamma^2 - u^2}. \tag{21}$$

In this paper we assume that heating takes place deep inside the disk at the midplane and in the atmosphere where $q^+ = 0$. However, it is straightforward to consider more general cases, where, e.g., the heating q^+ is proportional to the gas density, ρ (cf. Fukue 2005a, b).

We solved equations (18)–(21) for appropriate boundary conditions at the moving surface with a variable Eddington factor (13).

2.2. Boundary Conditions

As already pointed out in Fukue (2005a), the usual boundary conditions for the static atmosphere cannot be used for the present radiative flow, which moves with a velocity on the order of the speed of light.

When there is no motion in the gas ("static photosphere"), the radiation field just above the surface under the plane-parallel approximation is easily obtained. Namely, just above the disk with surface intensity I_{s}, the radiation energy density, E_{s}, the radiative flux, F_{s}, and the radiation pressure, P_{s} are $(2/c)\pi I_{\mathrm{s}}$, πI_{s}, and $(2/3c)\pi I_{\mathrm{s}}$, respectively, where the subscript s denotes the values at the disk surface. However, the radiation field just above the surface changes when the gas itself does move upward ("moving photosphere"), since the direction and intensity of radiation change due to relativistic aberration and Doppler effect (cf. Kato et al. 1998; Fukue 2000).

Let us suppose a situation where a flat infinite photosphere with surface intensity I_{s} in the comoving frame is not static, but moving upward at a speed v_{s} ($= c\beta_{\mathrm{s}}$, and the corresponding Lorentz factor is γ_{s}). Then, just above the surface, the radiation energy density, E_{s}, the radiative flux, F_{s}, and the radiation pressure, P_{s}, measured in the inertial frame become, respectively,

$$cE_{\mathrm{s}} = 2\pi I_{\mathrm{s}} \frac{3\gamma_{\mathrm{s}}^2 + 3\gamma_{\mathrm{s}} u_{\mathrm{s}} + u_{\mathrm{s}}^2}{3}, \tag{22}$$

$$F_{\mathrm{s}} = 2\pi I_{\mathrm{s}} \frac{3\gamma_{\mathrm{s}}^2 + 8\gamma_{\mathrm{s}} u_{\mathrm{s}} + 3u_{\mathrm{s}}^2}{6}, \tag{23}$$

$$cP_{\mathrm{s}} = 2\pi I_{\mathrm{s}} \frac{\gamma_{\mathrm{s}}^2 + 3\gamma_{\mathrm{s}} u_{\mathrm{s}} + 3u_{\mathrm{s}}^2}{3}, \tag{24}$$

where u_{s} ($= \gamma_{\mathrm{s}} v_{\mathrm{s}}/c$) is the flow four velocity at the surface (Fukue 2005a).

Thus, we impose the following boundary conditions: At the flow base (deep "inside" the atmosphere) with an arbitrary optical depth, τ_0, the flow velocity u is zero, the radiative flux is F_0 (which is a measure of the strength of radiation field), and the radiation pressure is P_0 (which connects with the radiation pressure gradient and relates to the internal structure), where the subscript 0 denotes the values at the flow base. At the flow top ("surface" of the atmosphere) where the optical depth is zero, the radiation field should satisfy the values above a moving photosphere given by equations (22)–(24): i.e.,

$$\frac{cP_{\mathrm{s}}}{F_{\mathrm{s}}} = \frac{2 + 6\beta_{\mathrm{s}} + 6\beta_{\mathrm{s}}^2}{3 + 8\beta_{\mathrm{s}} + 3\beta_{\mathrm{s}}^2}, \tag{25}$$

where β_{s} is a final speed at the disk surface.

Physically speaking, in the radiative flow starting from the flow base with an arbitrary optical depth, τ_0, for initial values of F_0 and P_0 at the flow base, the final value of the flow velocity, v_{s} at the flow top can be obtained by solving basic equations. Furthermore, the mass-loss rate J is determined as an eigenvalue so as to satisfy the boundary condition (23) at the flow top (cf. Fukue 2005a in the subrelativistic regime).

However, the permitted region for J is very tight, and it is difficult to search the value of J. Hence, in this paper, as a mathematically equivalent way, we fix the value of J, and search for the value of P_0 so as to satisfy the boundary condition (23).

3. Relativistic Radiative Flow under Gravity

In this section we show the relativistic radiative vertical flow in the luminous disk under the influence of gravity of the central object. In order to obtain the solution, as already stated, we numerically solved equations (18)–(21), starting from $\tau = \tau_0$ at $z = 0$ with appropriate initial conditions for v, F, and P, down to $\tau = 0$ so as to satisfy the boundary conditions (25) there. The parameters were the initial radius, r, on the disk, the initial optical depth, τ_0, which relates to the disk surface density, the initial flux F_0, which is the measure of the strength of radiation field to gravity, and the initial radiation pressure P_0 at the disk base, which connects with the radiation pressure gradient in the vertical direction and relates to the disk internal structure. The mass-loss rate J was determined as an eigenvalue of the boundary condition at the flow top.

Several examples of numerical calculations are shown in figures 1–3. The physical quantities were normalized in terms of the speed of light, c, the Schwarzschild radius, r_{g}, and the Eddington luminosity, L_{E} [$= 4\pi cGM/(\kappa_{\mathrm{abs}} + \kappa_{\mathrm{sca}})$]. The units of F, cP, and $c^2 J$ are $L_{\mathrm{E}}/(4\pi r_{\mathrm{g}}^2)$. It should be noted that the solutions can be obtained for arbitrary optical depths, τ_0,
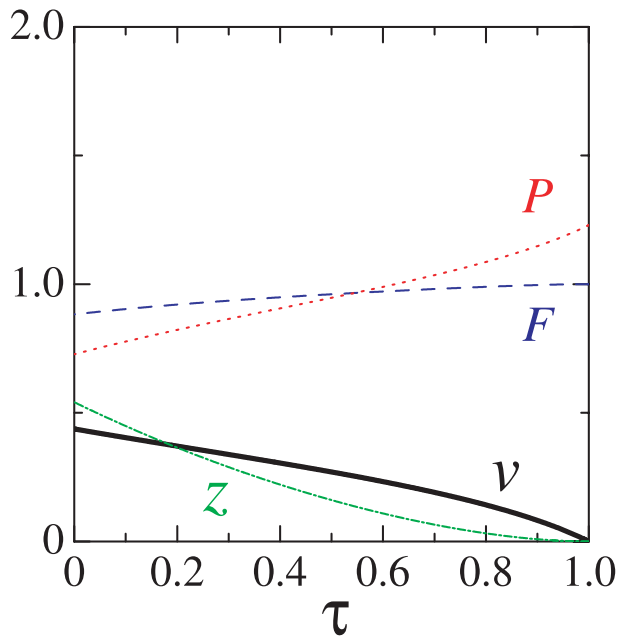
Fig. 1. Flow velocity v (thick solid curve), flow height z (chain-dotted one), radiative flux F (dashed one), and radiation pressure P (dotted one), as a function of the optical depth τ. The parameters are $r = 3$, $\tau_0 = 1$, $F_0 = 1$, and $P_0 = 1.23$. The mass-loss rate is $J = 1$. The quantities are normalized in units of c, r_g, and $L_E/(4\pi r_g^2)$.
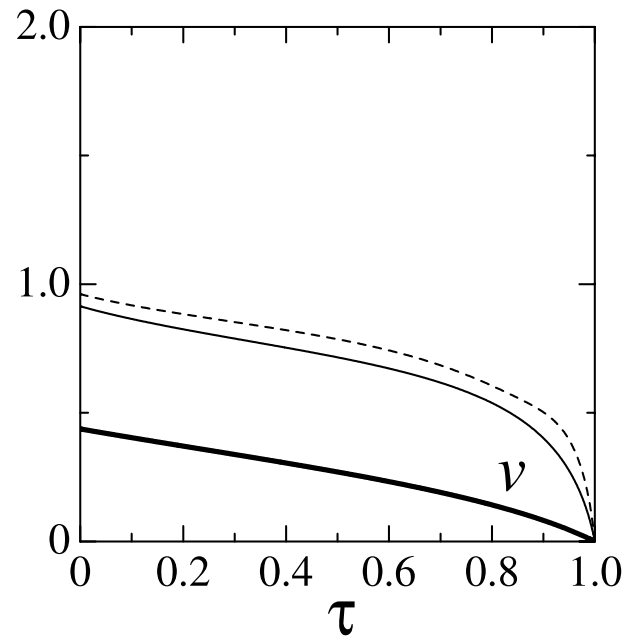

Fig. 2. Flow velocity v as a function of the optical depth τ. A thick solid curve is for the typical case of $r = 3$, $\tau_0 = 1$, $F_0 = 1$, and $P_0 = 1.23$ (i.e., $J = 1$). The solid curve is for the case of $r = 3$, $\tau_0 = 1$, $F_0 = 10$, and $P_0 = 10.6$ (i.e., $J = 1$), while the dashed one is for the case of $r = 3$, $\tau_0 = 1$, $F_0 = 1$, and $P_0 = 1.041$ (i.e., $J = 0.005$). The quantities are normalized in units of c, r_g, and $L_E/(4\pi r_g^2)$.

at the flow base (see Fukue 2006b, and section 4). We here show, however, the cases of $\tau_0 = 1$, where the velocity change is remarkable.

In figure 1 we show the flow velocity v (solid curve), the flow height z (chain-dotted one), the radiative flux F (dashed one), and the radiation pressure P (dotted one), as a function of the optical depth τ for $r = 3$, $\tau_0 = 1$, $F_0 = 1$, and $P_0 = 1.23$ (i.e., $J = 1$).

As the optical depth decreases from the flow base at the disk equator to the flow top at the disk surface, the radiative flux slightly decreases while the flow velocity increases; the radiative energy is converted to the flow bulk motion in the vertical direction. As is usually known, in a static plane-parallel atmosphere, under the radiative equilibrium with the gray approximation, the vertical flux, F, is conserved without any heating source. In the present relativistically *moving atmosphere*, on the contrary, the radiative flux, F, decreases via the Fu term, which acts to drive the gas toward the vertical direction. In the case of figure 1, the initial flux ($F_0 = 1$) is nearly the local Eddington one, and therefore, the final flow velocity is mildly relativistic due to the effect of gravity of the central object. Other parameter dependences are shown in figures 2 and 3.

In figure 2 the flow velocity v is shown for several parameter set: The thick solid curve is for the typical case of $r = 3$, $\tau_0 = 1$, $F_0 = 1$, and $P_0 = 1.23$ (i.e., $J = 1$). The solid curve is for the case of $r = 3$, $\tau_0 = 1$, $F_0 = 10$, and $P_0 = 10.6$ (i.e., $J = 1$), while the dashed one is for the case of $r = 3$, $\tau_0 = 1$, $F_0 = 1$, and $P_0 = 1.041$ (i.e., $J = 0.005$).

As is easily expected, the flow velocity remarkably increases when the initial flux, F_0, is large (a solid curve). When the initial flux is small, on the other hand, the flow velocity becomes small.

Even for the same initial flux, when the mass-loss rate is small, the flow velocity remarkably increases (a dashed curve). This is because for a small mass-loss rate the density decreases, and therefore the vertical height, z, becomes large, compared with the case for a large mass-loss rate with the same optical depth. As a result, the gas is accelerated along the long distance to reach the highly relativistic regime.

In figure 3 the dependence on the initial radius r is shown: $r = 3$ (a thick solid curve), $r = 2$ (a solid one), and $r = 1.5$ (a dashed one). Other parameters are $\tau_0 = 1$, $F_0 = 1$, and $P_0 = 1.23$ (i.e., $J = 1$).

For the same initial conditions, the flow velocity decreases as the initial radius decreases. This is just the effect of gravity of the central object. In the case of $r = 1.5$, the velocity is slightly *decelerated* toward the surface due to gravity.

4. Relativistic Radiative Flow in the Critical Disk

In this section we apply the present model to the mass outflow in the luminous supercritical accretion disks (cf. Fukue 2006a for a subrelativistic case).

When the mass-accretion rate, $\dot{M}$, in the disk around a central object of mass M highly exceeds the critical rate, $\dot{M}_{crit}$, defined by $\dot{M}_{crit} \equiv L_E/c^2$, the disk is believed to be in the supercritical regime, and the disk luminosity exceeds the Eddington one. Such a supercritical accretion disk, a so-called slim disk, has been extensively studied, both numerically
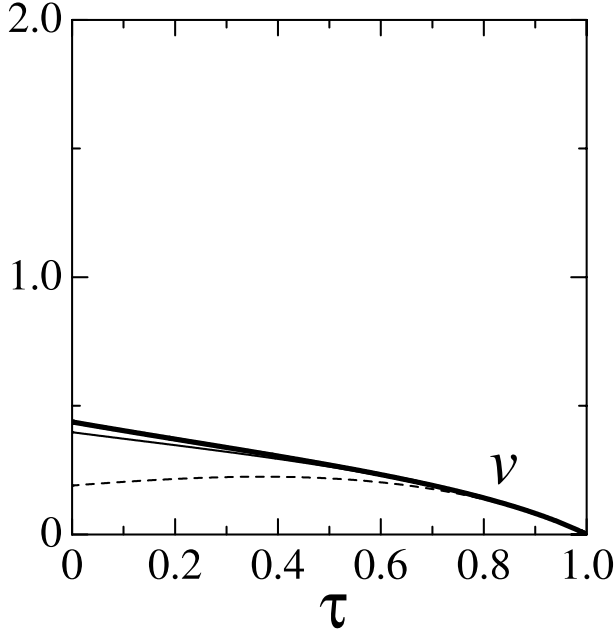
Fig. 3. Flow velocity, v, as a function of the optical depth, τ, for several initial radii r: $r = 3$ (a thick solid curve), $r = 2$ (a solid one), and $r = 1.5$ (a dashed one). The other parameters are $\tau_0 = 1$, $F_0 = 1$, and $P_0 = 1.23$ (i.e., $J = 1$). The quantities are normalized in units of c, r_g, and $L_E/(4\pi r_g^2)$.

and analytically (Abramowicz et al. 1988; Eggum et al. 1988; Szuszkiewicz et al. 1996; Beloborodov 1998; Watarai, Fukue 1999; Watarai et al. 2000; Mineshige et al. 2000; Fukue 2000; Kitabatake et al. 2002; Okuda 2002; Ohsuga et al. 2002, 2003, 2005; Watarai, Mineshige 2003; Fukue 2004; Ohsuga 2006). It was found that the optically-thick supercritical disk is roughly expressed by a self-similar model (e.g., Watarai, Fukue 1999; Fukue 2000; Kitabatake et al. 2002; Fukue 2004). Except for the case of Fukue (2004), however, many of these analytical models did not consider the mass outflow from the disk surface. Hence, in this paper we adopt a model developed by Fukue (2004), as a background supercritical disk model.

In the *critical accretion disk* constructed by Fukue (2004), the mass-accretion rate is assumed to be regulated just at the critical rate with the help of wind mass-loss. Outside some critical radius, the disk is in a radiation-pressure dominated standard state, while inside the critical radius the disk is in a critical state, where the excess mass is expelled by wind and the accretion rate is kept to be just at the critical rate at any radius. Here, the critical radius is derived as

$$r_{cr} = \frac{9\sqrt{3}\sigma_T}{16\pi m_p c} \dot{M}_{input} \sim 1.95 \dot{m}\, r_g, \tag{26}$$

where $\dot{M}_{input}$ is the accretion rate at the outer edge of the disk, and $\dot{m} = \dot{M}_{input}/\dot{M}_{crit}$. Outside r_{cr}, the accretion rate is constant, while inside r_{cr} the accretion rate would vary as

$$\dot{M}(r) = \frac{16\pi c m_p}{9\sqrt{3}\sigma_T} r = \dot{M}_{input} \frac{r}{r_{cr}}. \tag{27}$$

In such a critical accretion disk, the disk thickness, H, is conical as

$$\frac{H}{r} = \sqrt{c_3} = \frac{1}{4}\ln\left(1 + \frac{\dot{m}}{20}\right), \tag{28}$$

where c_3 is some numerical coefficient determined by the similar procedure in Narayan and Yi (1994) for optically-thin advection-dominated disks. The second equality of this relation comes from a numerical calculation (Watarai et al. 2000). Although the mass loss was not considered in Watarai et al. (2000), we adopted this relation as some measure: when the normalized accretion rate $\dot{m}$ is 1000, the coefficient $\sqrt{c_3}$ becomes 0.983.

Furthermore, in Fukue (2004), several alternatives are discussed, and some of them gives the physical quantities of the critical accretion disk with mass loss as

$$\tau_0 = \frac{16\sqrt{6}}{\alpha}\sqrt{\frac{r}{r_g}}, \tag{29}$$

$$F_0 = \frac{12\sqrt{6}}{\alpha}\sqrt{c_3}\frac{L_E}{4\pi r^2}\sqrt{\frac{r}{r_g}}, \tag{30}$$

$$cP_0 = \frac{cGM}{\kappa}\sqrt{c_3}\tau_0\frac{1}{r^2} = \frac{16\sqrt{6}\,c\,GM}{\alpha\kappa}\sqrt{c_3}\frac{1}{r^2}\sqrt{\frac{r}{r_g}}, \tag{31}$$

where α is the viscous parameter.

In the present non-dimensional unit in terms of c, r_g, and the Eddington luminosity L_E, these physical quantities are expressed as

$$H = \sqrt{c_3}\,r, \tag{32}$$

$$\tau_0 = \frac{16\sqrt{6}}{\alpha}\sqrt{r}, \tag{33}$$

$$F_0 = \frac{12\sqrt{6}}{\alpha}\sqrt{c_3}\frac{1}{r^{3/2}}, \tag{34}$$

$$P_0 = \frac{16\sqrt{6}}{\alpha}\sqrt{c_3}\frac{1}{r^{3/2}}, \tag{35}$$

where the symbol "hat" (say, $\hat{r}$) is dropped.

Using these relations, we can solve the basic equations, and obtain numerical solutions at each radius r. The example in the case of $\dot{m} = 1000$ and $\alpha = 1$ is shown in figures 4 and 5.

In figure 4 we show the flow velocity v as a function of optical depth, τ, for several values of r. The quantities are normalized in units of c and r_g. The parameters of the critical disk are $\dot{m} = 1000$ and $\alpha = 1$.

As can be seen in figure 4, the flow velocity, v, varies self-similarly for different values of the radii. This may be reflected the initial self-similar models. As a result, in each radius with different optical depth, the flow final speed is almost the same.

In figure 5 we show several quantities for each radius r: The disk height, H (dashed curve), and the optical depth, τ_0 (chain-dotted one), are from the critical accretion disk model, while the height, z_s, and velocity, v_s (solid curves), at the flow top and the mass-loss rate, J (dashed one), are the results of numerical calculations. The quantities are normalized in units of c and r_g. The parameters of the critical disk is $\dot{m} = 1000$ and $\alpha = 1$.

As can be seen in figure 5, the flow height, z_s, is enormously large. Hence, rigorously speaking, the present plane-parallel
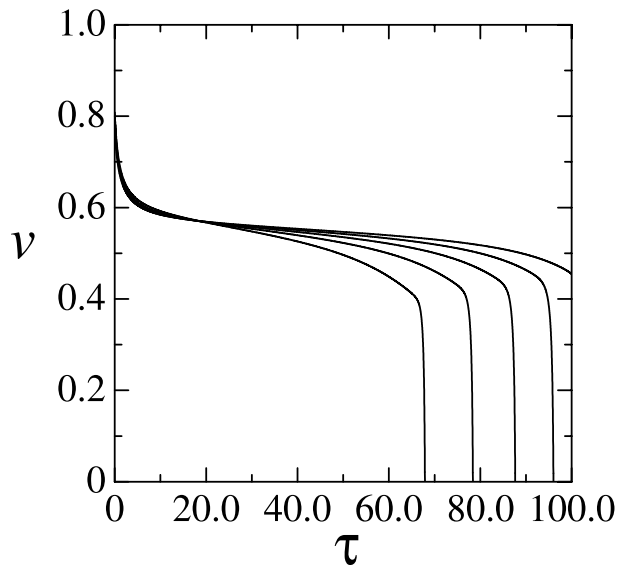
Fig. 4. Flow velocity, v, as a function of τ for several values of r. The values of r are, from left to right, 3, 4, 5, 6, and 7. The quantities are normalized in units of c and $r_{\rm g}$. The parameters of the critical disk is $\dot{m} = 1000$ and $\alpha = 1$.
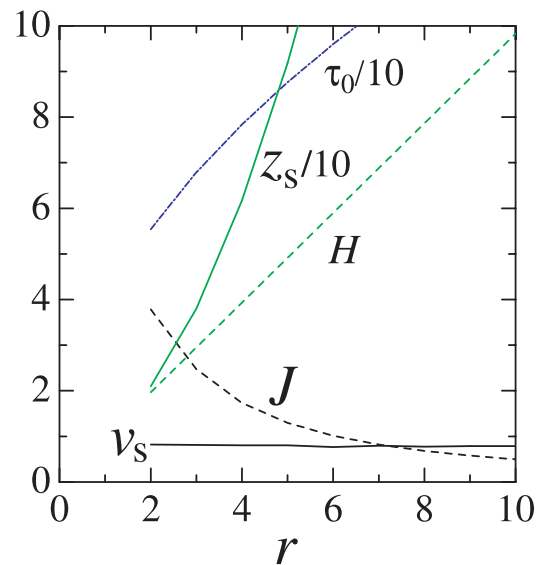

Fig. 5. Several quantities for each radius r: The disk height, H (dashed curve), and the optical depth, τ, (chain-dotted one) are from the critical model, while the height, $z_{\rm s}$, and velocity, $v_{\rm s}$ (solid curves), at the flow top and the mass-loss rate, J (dashed one), are the results of the present numerical calculations. The quantities are normalized in units of c and $r_{\rm g}$. The parameters of the critical disk is $\dot{m} = 1000$ and $\alpha = 1$.

approximation violates in this application of $\dot{m} = 1000$, and two-dimensional numerical simulation should be needed in such a case. However, we can see several insights from the present case.

First, the final speed of the flow accelerated in the luminous critical disk becomes sufficiently relativistic. In other words, relativistic jets can form in such a luminous accretion disk. In addition, this final speed does not depend on the initial radius very much, perhaps due to the initial self-similarity. Second, on the contrary to the final speed, the mass-loss rate per unit area increases as the initial radius decreases; it is roughly approximated by $J \sim 6/r$. On the other hand, the model mass-loss rate (Fukue 2004, 2006a) becomes $J = 1/r$, that is qualitatively same, but quantitatively different from the present numerical values. Hence, the mass loss from the critical disk may be concentrated in the inner region, although the true mass-loss rate cannot be determined at the present simple state. This nature, however, is also convenient for centrally concentrated jets.

5. Concluding Remarks

In this paper we have examined the relativistic radiative transfer flow in a luminous disk in the relativistic regime of $(v/c)^2$, while taking account of the gravity of the central object. In such a relativistic regime, we adopted the velocity-dependent variable Eddington factor. The flow was assumed to be vertical, and the gas pressure was ignored for simplicity. The basic equations were numerically solved as a function of the optical depth, τ, and the flow velocity, v, the height, z, the radiative flux, F, and the radiation pressure, P, were obtained for a given radius, r, the initial optical depth, τ_0, and the initial conditions at the flow base (disk "inside"), whereas the mass-loss rate, J, was determined as an eigenvalue of the boundary condition at the flow top (disk "surface"). For sufficiently

luminous cases, the flow resembles the case without gravity. For less-luminous cases, however, the flow velocity decreases.

Application to the critical accretion disk was also examined. If the disk thickness becomes so large, the present plane-parallel approximation violates and other treatment, such as numerical simulations, should be needed.

The radiative flow investigated in the present paper must be a quite *fundamental problem* for accretion-disk physics and astrophysical jet formation, although there are many simplifications at the present stage. For example, we have ignored the gas pressure. In general cases, where the gas pressure is considered, there usually appears sonic points, and the flow is accelerated from subsonic to supersonic. In this paper we considered a purely vertical flow, and the cross section of the flow is constant. If the cross section of the flow increases along the flow, the flow properties, such as the transonic nature, would be influenced. Moreover, we did not consider the rotation of the gas. In accretion disks around a black hole, the gas usually rotates around the hole at relativistic speeds. In the vicinity of the equator, the vertical flow approximation safely holds, since the radial gravity is balanced with the centrifugal force. When the flow is accelerated to be lifted up to a large height, the streamline would be curved outward, since the centrifugal force dominates. This would violate the vertical flow approximation.

There remain many problems to be solved.

References

Abramowicz, M. A., Czerny, B., Lasota, J. P., & Szuszkiewicz, E. 1988, ApJ, 332, 646

Adam, J., Störzer, H., Shaviv, G., & Wehrse, R. 1988, A&A, 193, L1

Artemova, I. V., Bisnovatyi-Kogan, G. S., Björnsson, G., & Novikov, I. D. 1996, ApJ, 456, 119

Beloborodov, A. M. 1998, MNRAS, 297, 739

Bisnovatyi-Kogan, G. S., & Blinnikov, S. I. 1977, A&A, 59, 111

Cannizzo, J. K., & Wheeler, J. C. 1984, ApJS, 55, 367

Davis, S. W., Blaes, O. M., Hubeny, I., & Turner, N. J. 2005, ApJ, 621, 372

Dullemond, C. P. 1999, A&A, 343, 1030

Eggum, G. E., Coroniti, F. V., & Katz, J. I. 1985, ApJ, 298, L41

Eggum, G. E., Coroniti, F. V., & Katz, J. I. 1988, ApJ, 330, 142

Fukue, J. 2000, PASJ, 52, 829

Fukue, J. 2004, PASJ, 56, 569

Fukue, J. 2005a, PASJ, 57, 841

Fukue, J. 2005b, PASJ, 57, 1023

Fukue, J. 2006a, PASJ, 58, 187

Fukue, J. 2006b, PASJ, 58, 461

Fukue, J., Tojyo, M., & Hirai, Y. 2001, PASJ, 53, 555

Hirai, Y., & Fukue, J. 2001, PASJ, 53, 285

Hubeny, I. 1990, ApJ, 351, 632

Hubeny, I., Agol, E., Blaes, O., & Krolik, J. H. 2000, ApJ, 533, 710

Hubeny, I., Blaes, O., Krolik, J. H., & Agol, E. 2001, ApJ, 559, 680

Hubeny, I., & Hubeny, V. 1997, ApJ, 484, L37

Hubeny, I., & Hubeny, V. 1998, ApJ, 505, 558

Hui, Y., Krolik, J. H., & Hubeny, I. 2005, ApJ, 625, 913

Icke, V. 1980, AJ, 85, 329

Kato, S., Fukue, J., & Mineshige, S. 1998, Black-Hole Accretion Disks (Kyoto: Kyoto University Press)

Katz, J. I. 1980, ApJ, 236, L127

Kitabatake, E., Fukue, J., & Matsumoto, K. 2002, PASJ, 54, 235

Melia, F., & Königl, A. 1989, ApJ, 340, 162

Meyer, F., & Meyer-Hofmeister, E. 1982, A&A, 106, 34

Mineshige, S., Kawaguchi, T., Takeuchi, M., & Hayashida, K. 2000, PASJ, 52, 499

Misra, R., & Melia, F. 1993, ApJ, 419, L25

Narayan, R., & Yi, I. 1994, ApJ, 428, L13

Ohsuga, K. 2006, ApJ, 640, 923

Ohsuga, K., Mineshige, S., Mori, M., & Umemura, M. 2002, ApJ, 574, 315

Ohsuga, K., Mineshige, S., & Watarai, K. 2003, ApJ, 596, 429

Ohsuga, K., Mori, M., Nakamoto, T., & Mineshige, S. 2005, ApJ, 628, 368

Okuda, T. 2002, PASJ, 54, 253

Orihara, S., & Fukue, J. 2003, PASJ, 55, 953

Paczyński, B., & Wiita, P. J. 1980, A&A, 88, 23

Ross, R. R., Fabian, A. C., & Mineshige, S. 1992, MNRAS, 258, 189

Shaviv, G., & Wehrse, R. 1986, A&A, 159, L5

Szuszkiewicz, E., Malkan, M. A., & Abramowicz, M. A. 1996, ApJ, 458, 474

Tajima, Y., & Fukue, J. 1996, PASJ, 48, 529

Tajima, Y., & Fukue, J. 1998, PASJ, 50, 483

Tamazawa, S., Toyama, K., Kaneko, N., & Ôno, Y. 1975, Ap&SS, 32, 403

Turolla, R., & Nobili, L. 1988, MNRAS, 235, 1273

Turolla, R., Zampieri, L., & Nobili, L. 1995, MNRAS, 272, 625

Watarai, K., & Fukue, J. 1999, PASJ, 51, 725

Watarai, K., Fukue, J., Takeuchi, M., & Mineshige, S. 2000, PASJ, 52, 133

Watarai, K., & Mineshige, S. 2003, PASJ, 55, 959